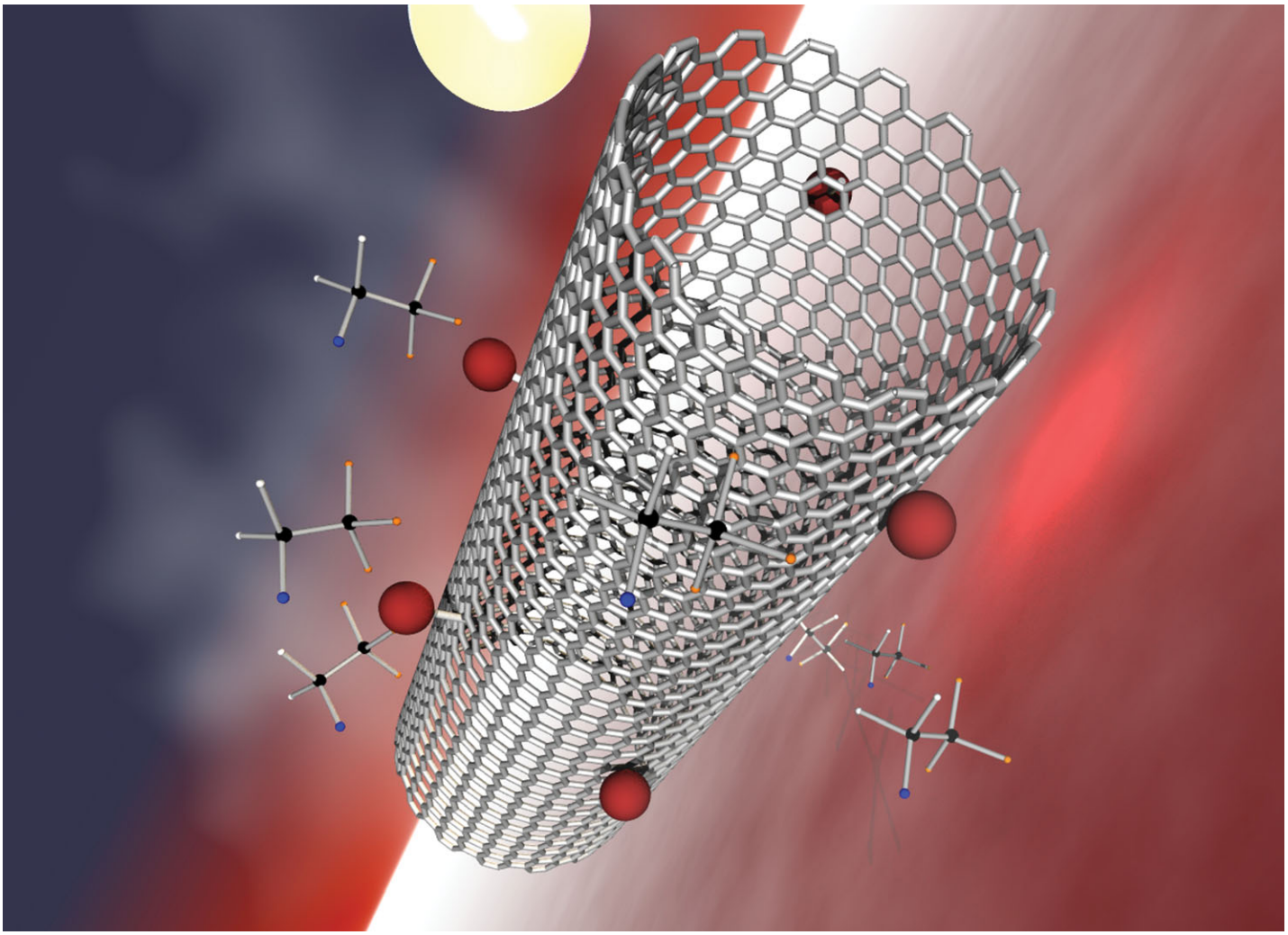

Showcasing research in Andreas Hirsch's Laboratory, Department of Chemistry and Pharmacy, Friedrich-Alexander-Universität Erlangen-Nürnberg, Germany

Brominated single walled carbon nanotubes as versatile precursors for covalent sidewall functionalization

The facile preparation of brominated SWCNTs based on two complementary reductive activation routes is reported. The brominated SWCNTs are highly reactive and can be used in nucleophilic substitution reactions and represent versatile starting materials for the generation of sidewall functionalized SWCNTs with a high density of functional moieties.

As featured in:

See Andreas Hirsch *et al.*, *Chem. Commun.*, 2014, **50**, 6582.

ROYAL SOCIETY OF CHEMISTRY

www.rsc.org/chemcomm

Registered charity number: 207890

ChemComm

COMMUNICATION

View Article Online
View Journal | View Issue

Cite this: *Chem. Commun.*, 2014, **50**, 6582

Received 27th January 2014,
Accepted 4th March 2014

DOI: 10.1039/c4cc00719k

www.rsc.org/chemcomm

Brominated single walled carbon nanotubes as versatile precursors for covalent sidewall functionalization†

Ferdinand Hof, Frank Hauke and Andreas Hirsch*

Herein we report on the facile preparation of brominated SWCNTs based on two complementary reductive activation routes. The respective brominated SWCNTs are highly reactive and can be used in nucleophilic substitution reactions and represent versatile starting materials for the generation of sidewall functionalized SWCNTs with a high density of functional moieties.

In the last decade, chemistry of single walled carbon nanotubes (SWCNTs) has attracted a lot of interest with respect to covalent framework functionalization and functional group conversion.[1,2] In this context, remarkable progress has been made, both in the sense of the exploration of the chemical reactivity of SWCNTs[3–6] as well as in terms of the analytical product characterization.[7,8] Nevertheless, the establishment of highly functional organic moieties, covalently connected with the carbon nanotube framework, still remains challenging and is primarily based on stepwise reaction pathways, utilizing carbon nanotube derivatives with covalently attached anchor groups, *e.g.* hydroxyl functionalities.[9] Due to the low intrinsic reactivity of SWCNTs relatively harsh reaction conditions are needed for covalent framework addition reactions. As a consequence, successfully attached functional entities are limited to carboxyl groups,[10,11] phenyl-[12,13] or alkyl addends[14] or hydroxyl functionalities.[15] In contrast to addition reactions, nucleophilic SWCNT substitution reactions have hardly been investigated and are solely based on fluorinated carbon nanotube precursors.[16–18] For instance, Stevens *et al.* have shown that fluorine substituents on SWCNTs can be substituted by alkyl groups from Grignard and alkyllithium reagents.[19] The main disadvantage of using fluorinated carbon nanotubes as precursors in SWCNT substitution reactions is their relatively harsh formation conditions, which do not allow easy control of the degree of addition. In principle, other halogenated carbon nanotubes, like brominated[20,21] or iodinated[22] SWCNTs, are also accessible but these systems have not been used for subsequent derivatization reactions.

Here, we report on the synthesis and unambiguous characterization of brominated SWNCTs in combination with a subsequent nucleophilic substitution approach (Scheme 1). The key step of this straightforward synthetic approach was the use of reduced $SWCNT^{n-}$ as highly reactive intermediates. The reductive activation of the SWCNT (HiPco) starting material was achieved by two different approaches: (a) molten potassium metal based reduction, leading to the formation of the species **1a**[5] or (b) Birch type reduction[12,14,23] with potassium dissolved in liquid ammonia, yielding species **1b**.[12] This initial reduction step is a fundamental prerequisite which leads to an efficient SWCNT individualization and charge induced reactivity increase for the subsequent bromine addition. The respective brominated SWCNTs **2a**, **2b** represent highly reactive species. We have found that the addition of water leads to an efficient nucleophilic substitution of the covalently bound sidewall bromine atoms and to the formation of hydroxylated SWCNT derivatives. Because of this pronounced reactivity a detailed Raman spectroscopic characterization of the brominated SWCNTs **2a**, **2b** has been carried out under inert gas conditions, following a procedure that we have recently published.[5] In order to gain a statistically significant bulk information about the success of the covalent functionalization of the reductively activated SWCNT intermediates with bromine **2a**, **2b**, Scanning Raman Microscopy (SRM) was performed and the respective $I_{(D/G)}$ (intensity ratios of the D- and G-bands) values of the recorded 625 individual Raman spectra were plotted as a distribution function (Fig. 1).

In general, the D-band intensity is a measure of the amount of sp^3-defects introduced by covalent addend binding. As it can be clearly seen from Fig. 1, sidewall brominated SWCNTs are accessible by both reaction pathways, with a mean $I_{(D/G)}$ ratio of about 0.5 by solid state reduction with potassium and 0.4 in the case of Birch type reduction. The corresponding distribution functions for λ_{exc} = 532 nm and λ_{exc} = 785 nm are depicted in Fig. S1 (ESI†). Use of additional excitation energies and organizing

Department of Chemistry and Pharmacy and Institute of Advanced Materials and Processes (ZMP), Friedrich-Alexander-Universität Erlangen-Nürnberg (FAU), Henkestrasse 42, 91054 Erlangen, Germany. E-mail: andreas.hirsch@fau.de; Fax: +49 9131-8526864; Tel: +49 9131-8522537

† Electronic supplementary information (ESI) available: Experimental details regarding the synthesis of different SWCNT derivatives, additional Raman analysis and TG/MS data. See DOI: 10.1039/c4cc00719k

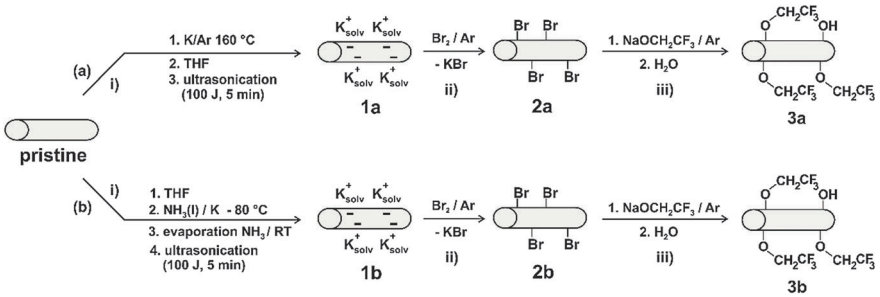

Scheme 1 Sidewall alkoxide functionalization of SWCNTs *via* (i) reduction with molten potassium (pathway a) or Birch type reduction (pathway b) to the corresponding carbon nanotubes **1a** and **1b** followed by (ii) bromination to the synthetic precursor building blocks **2a** and **2b** and (iii) subsequent nucleophilic substitution with $NaOCH_2CF_3$ yielding alkoxides **3a** and **3b**, respectively.

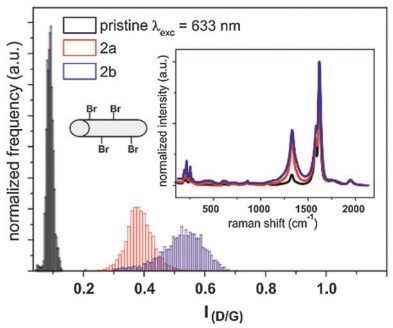

Fig. 1 Statistical Raman analysis of the brominated SWCNT adducts **2a** and **2b**; λ_{exc} = 633 nm. Inset: median spectra.

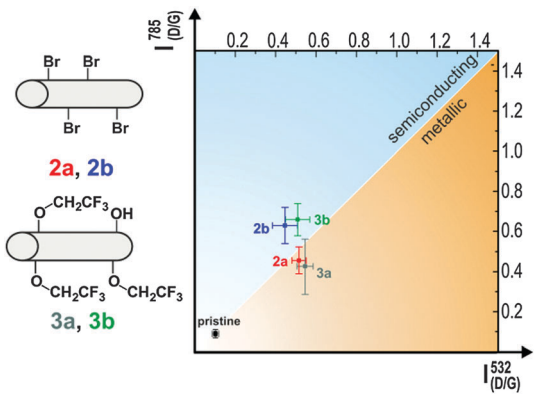

Fig. 2 2-D Raman index plot based on the statistical Raman analysis of the samples **2a**, **2b**, **3a**, **3b** at λ_{exc} = 532 nm and λ_{exc} = 785 nm. – For detailed data see Table T1 – ESI.†

the measured data in a 2D-diagram (Fig. 2) provide valuable information about the homogeneity distribution (Raman Homogeneity Index (RHI)) and the electronic type selectivity (Raman Selectivity Index (RSI)) of the initial addition reaction (see also Table T1 – ESI†).[8]

In contrast to pathway (a), where no selectivity is observed (RSI = 1.9°), the Birch type based addition sequence (b) exhibits a RSI value of 12.3°, indicative of a selectivity with respect to semiconducting SWCNTs. This kind of electronic type selectivity has also been observed with other Birch type based functionalization sequences.[11] The Raman based analysis provides a direct

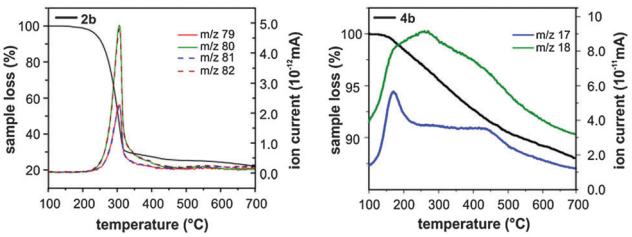

Fig. 3 TG/MS profiles of brominated SWCNTs **2b** (left) and hydroxylated SWCNTs **4b** (right).

insight into the introduction of sp^3-defects, but does not lead to any information about the chemical nature of the bound addends. For this purpose, the brominated SWCNT derivative **2b** was analysed by means of thermogravimetric analysis coupled with mass spectrometry (TG/MS) – (Fig. 3 – left). Here, a sharp mass loss (Δwt = 71% – corrected by mass loss of the pristine starting material – ESI,† Fig. S3) is detected in the region between 250 and 350 °C and can be traced back to the detachment of bromine from the mass fragments *m*/*z* 79, 81 (*m*/*z* 80, 82 [HBr]) based on its characteristic isotopic distribution (1 : 1). For **2b**, a degree of functionalization of about 5% can be calculated. The covalently bound bromine addends can easily and quantitatively be substituted by the addition of water (Scheme 2).

This reaction sequence provides a fast access route to hydroxylated SWCNT derivatives **4b**. The detached bromide ions were identified in the aqueous phase by precipitating as silver bromide. The TG/MS analysis of **4b** (Fig. 3 – right) corroborated the substitution of the bromo addends. The introduced hydroxyl groups can be identified by their mass fragments *m*/*z* 17, 18 (further mass traces see Fig. S4, ESI†) and a sample mass loss of about 8% (after correction – see Fig. S3, ESI†) is detected – no remaining bromine was found for **4b**. Based on these data, the degree of functionalization before and after hydrolysis is determined to be about 5% and it

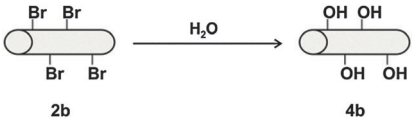

Scheme 2 Hydrolysis of brominated SWCNT intermediates, yielding sidewall hydroxylated SWCNT derivatives **4b**.

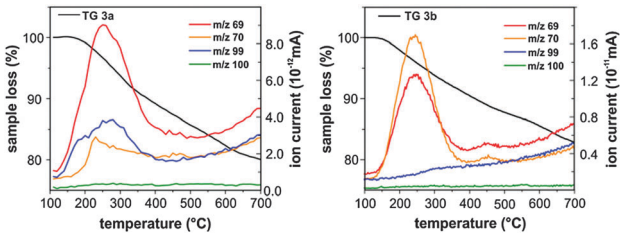

Fig. 4 TG/MS profiles of final substitution products **3a** (left) and **3b** (right).

remains practically unchanged which is indicative of a quantitative substitution of the bromine atoms.

Hydroxylated carbon nanotubes **4b** may serve as highly functionalized starting materials in subsequent coupling reactions with carboxylic acid derivatives; alternatively, the functional entity can directly be brought in by the reaction of brominated SWCNTs with functional alcoholates. The feasibility of this concept has been exemplarily proven by the reaction of **2a** and **2b** with 2,2,2-trifluoro ethanolate (Scheme 1). The trifluoro ethanol group serves as a suitable marker for the TG/MS analysis (Fig. 4). In the main mass loss region (100–400 °C, 9% corrected mass loss) all characteristic mass fragments of the trifluoro ethanol group were detected: *m/z* 69 $-CF_3$, *m/z* 70 HCF_3, *m/z* 99 F_3CCH_2O-, *m/z* 100 F_3CCH_2OH. Again, in both substitution products **3a** and **3b** no traces of bromine were detected by TG/MS, indicative of a quantitative substitution of the initially bound bromo addends.

This fact is furthermore corroborated by statistical Raman analysis of the final substitution products **3a** and **3b**. Here, it can be shown that the initial density of defects, present in the respective brominated SWCNT derivatives **2a** and **2b**, is virtually not increased after the addition of 2,2,2-trifluoro ethanolate (Fig. 2). Therefore, no additional carbon lattice sp^3 centers are introduced during this part of the functionalization sequence. Moreover, as can be clearly seen in the 2D-Raman index plot, the initial electronic type discrimination with respect to semiconducting SWCNT species (represented by the RSI values – Table T1, ESI†) remains unchanged by the subsequent substitution reaction. In a reference experiment we have also investigated whether the observed data can be traced back to a direct nucleophilic sidewall addition of 2,2,2-trifluoro ethanolate (Scheme S1, ESI†). Therefore, pristine HiPco SWCNTs were reacted with the alcoholate under the same reaction conditions as those used for the bromo substitution sequence. The respective Raman spectra and TG/MS data (Fig. S5, ESI†) unequivocally show that attachment of 2,2,2-trifluoro ethanolate does not take place. This clearly demonstrates that a nucleophilic substitution mechanism of brominated SWCNTs is responsible for the formation of the alkoxylated tubes **3a**, **3b**.

Brominated carbon nanotubes, accessible by a direct reductive bromination sequence, serve as versatile building blocks for the facile generation of sidewall functionalized SWCNT derivatives. Two complementary routes were used for the synthesis of these highly reactive intermediates: (a) solid state reduction of SWCNTs with potassium and (b) Birch type reduction with a subsequent reaction with bromine, respectively. The bromo addends are easily and quantitatively substituted by water or alcoholates *via* a nucleophilic substitution pathway. This process does not lead to an additional introduction of framework sp^3 centers, which is confirmed by Scanning Raman Microscopy (SRM). In the case of the Birch type reduction sequence, an electronic type selective framework functionalization with respect to semiconducting species is observed. Based on their easy access and high reactivity, brominated SWCNTs can serve as a versatile starting material for the generation of multifunctional SWCNT architectures for future applications. Research with respect to this goal is currently being pursued in our laboratory.

The authors thank the Deutsche Forschungsgemeinschaft (DFG – SFB 953, Project A1 "Synthetic Carbon Allotropes") and the Interdisciplinary Center for Molecular Materials (ICMM) for the financial support.

Notes and references

1 S. A. Hodge, M. K. Bayazit, K. S. Coleman and M. S. P. Shaffer, *Chem. Soc. Rev.*, 2012, **41**, 4409–4429.
2 V. Georgakilas, K. Kordatos, M. Prato, D. M. Guldi, M. Holzinger and A. Hirsch, *J. Am. Chem. Soc.*, 2002, **124**, 760–761.
3 Z. Syrgiannis, V. La Parola, C. Hadad, M. Lucío, E. Vázquez, F. Giacalone and M. Prato, *Angew. Chem., Int. Ed.*, 2013, **52**, 6480–6483.
4 B. Vanhorenbeke, C. Vriamont, F. Pennetreau, M. Devillers, O. Riant and S. Hermans, *Chem.–Eur. J.*, 2013, **19**, 852–856.
5 F. Hof, S. Bosch, S. Eigler, F. Hauke and A. Hirsch, *J. Am. Chem. Soc.*, 2013, **135**, 18385–18395.
6 C. Zhao, Y. Song, K. Qu, J. Ren and X. Qu, *Chem. Mater.*, 2010, **22**, 5718–5724.
7 M. S. Dresselhaus, A. Jorio, M. Hofmann, G. Dresselhaus and R. Saito, *Nano Lett.*, 2010, **10**, 751–758.
8 F. Hof, S. Bosch, J. M. Englert, F. Hauke and A. Hirsch, *Angew. Chem., Int. Ed.*, 2012, **51**, 11727–11730.
9 T. Palacin, H. L. Khanh, B. Jousselme, P. Jegou, A. Filoramo, C. Ehli, D. M. Guldi and S. Campidelli, *J. Am. Chem. Soc.*, 2009, **131**, 15394–15402.
10 H. Yu, Y. Jin, F. Peng, H. Wang and J. Yang, *J. Phys. Chem. C*, 2008, **112**, 6758–6763.
11 B. Gebhardt, F. Hof, C. Backes, M. Müller, T. Plocke, J. Maultzsch, C. Thomsen, F. Hauke and A. Hirsch, *J. Am. Chem. Soc.*, 2011, **133**, 19459–19473.
12 Y. Ying, R. K. Saini, F. Liang, A. K. Sadana and W. E. Billups, *Org. Lett.*, 2003, **5**, 1471–1473.
13 C. A. Dyke and J. M. Tour, *J. Phys. Chem. A*, 2004, **108**, 11151–11159.
14 F. Liang, A. K. Sadana, A. Peera, J. Chattopadhyay, Z. Gu, R. H. Hauge and W. E. Billups, *Nano Lett.*, 2004, **4**, 1257–1260.
15 B. Gebhardt, Z. Syrgiannis, C. Backes, R. Graupner, F. Hauke and A. Hirsch, *J. Am. Chem. Soc.*, 2011, **133**, 7985–7995.
16 L. Valentini, J. Macan, I. Armentano, F. Mengoni and J. M. Kenny, *Carbon*, 2006, **44**, 2196–2201.
17 L. Zhang, V. U. Kiny, H. Peng, J. Zhu, R. F. M. Lobo, J. L. Margrave and V. N. Khabashesku, *Chem. Mater.*, 2004, **16**, 2055–2061.
18 M. X. Pulikkathara, O. V. Kuznetsov and V. N. Khabashesku, *Chem. Mater.*, 2008, **20**, 2685–2695.
19 J. L. Stevens, A. Y. Huang, H. Peng, I. W. Chiang, V. N. Khabashesku and J. L. Margrave, *Nano Lett.*, 2003, **3**, 331–336.
20 J. F. Colomer, R. Marega, H. Traboulsi, M. Meneghetti, G. Van Tendeloo and D. Bonifazi, *Chem. Mater.*, 2009, **21**, 4747–4749.
21 W. Z. Wang, A. S. Mahasin, P. Q. Gao, K. H. Lim and M. B. Chan-Park, *J. Phys. Chem. C*, 2012, **116**, 23027–23035.
22 K. S. Coleman, A. K. Chakraborty, S. R. Bailey, J. Sloan and M. Alexander, *Chem. Mater.*, 2007, **19**, 1076–1081.
23 J. Chattopadhyay, S. Chakraborty, A. Mukherjee, R. Wang, P. S. Engel and W. E. Billups, *J. Phys. Chem. C*, 2007, **111**, 17928–17932.

